Numerical Simulation of a Knudsen Pump Using the Effect of Curvature of the Channel

K. Aoki[1], P. Degond[2], L. Mieussens[2], M. Nishioka[1], S. Takata[1]

[1]*Department of Mechanical Engineering and Science and*
Advanced Research Institute of Fluid Science and Engineering,
Kyoto University, Kyoto 606-8501, Japan
[2]*MIP, Université Paul Sabatier, 31062 Toulouse cedex, France*

Abstract. A feasibility of making a Knudsen pump by changing the curvature of the channel, instead of changing its cross-sectional area, is investigated numerically by the direct simulation Monte Carlo method. As a result, it is shown that a two-dimensional channel with a snaky shape, composed of alternately arranged straight and semicircular segments, with a periodic temperature distribution has a pumping effect.

INTRODUCTION

The Knudsen pump (or compressor) [1] is a pump without moving parts that works for a gas under rarefied conditions or in microscales. The typical Knudsen pump is a long channel with a periodic structure consisting of alternately arranged narrow and wide channels. The temperature of the channel wall is also periodic with the same period as the structure, such as a saw-like distribution increasing along the narrow channels and decreasing along the wide channels. Such a channel causes a unidirectional gas flow with a pumping effect. [A unidirectional flow with a pumping effect can be obtained straightforwardly by applying monotonically increasing temperature along the channel wall (thermal transpiration [3]); however, this results in a practical difficulty that an extremely large temperature difference must be imposed at both ends of the channel. The periodic temperature distribution of the Knudsen pump avoids this difficulty.] The flow and its pumping effect have been studied numerically [4, 5] by the direct simulation Monte Carlo (DSMC) method [6, 7] as well as experimentally [8, 9].

In the present study, we investigate the possibility of replacing the narrow segments with curved channels with the same width as the wide segments. In the present paper, we report on some numerical results obtained by the DSMC method for hard-sphere molecules and for the diffuse-reflection condition on the channel wall. It should be mentioned that, in parallel with the DSMC computation, we have also derived a diffusion-type model applicable to the present problem using the BGK model [10].

PROBLEMS

As the first step, we investigate the following problem.

Problem I: We consider a gas in a (two-dimensional) ring-shaped channel with a uniform width, consisting of two straight channels and two semi-circular channels [Fig. 1(a)]. Here, w is the width of the channel, L is the length of the straight segments, and R_c is the radius of the median line of the semi-circular segments. The temperature of the channel walls is kept at T_1 at the positions A and C and at T_0 ($< T_1$) at the positions B and D and is assumed to change linearly with the distance along the walls. We investigate the steady behavior of the gas in the circuit for a wide range of the Knudsen number.

As will be shown below, a circulating flow is induced in Problem I. Therefore, it may be possible to make a variant of the Knudsen compressor using a curved channel in place of a narrow segment. As the second step, we investigate the pumping effect of the circulating flow, considering the following problem.

Problem II: Consider a cascade system shown in Fig. 1(b) that is formed as follows. Let us define the basic unit P by the part ABC of the ring in Fig. 1(a) (together with the temperature distribution of the channel walls) and the basic
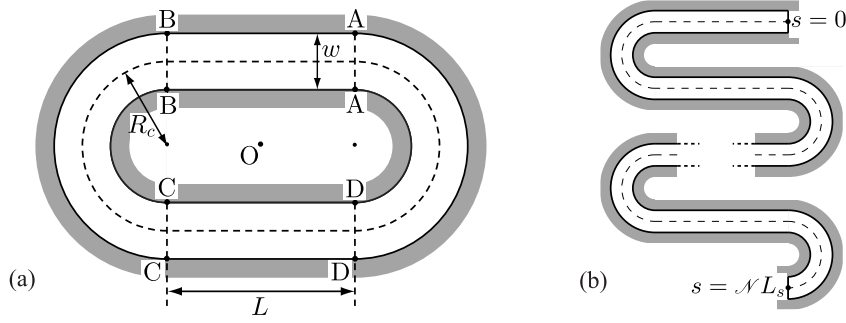
FIGURE 1. Geometries. (a) Ring-shaped channel, (b) Snaky cascade system.

unit P′ by the mirror image of the part CDA of the same ring, with respect to the median line of the part CD (together with the temperature distribution of the channel walls). Then, we join the basic units P and P′ alternately to form the cascade system. Then, we consider the case where both ends of the cascade system are closed by diffusely reflecting walls of temperature T_1 and investigate the steady pressure distribution along the channel.

In the present two-dimensional channel case, the cascade system corresponding to the one-way circulating flow induced in the ring in Problem I should be the snaky channel considered in Problem II. However, in the case of a pipe, which is not considered here, another cascade system can be made by rolling up the pipe helically. This geometry would be more interesting for practical applications. In any case, it should be emphasized that, if a certain pressure difference arises between both ends of the cascade system, one can make a pump only by bending a single channel or pipe appropriately and heating and cooling it at right positions.

RESULTS OF COMPUTATION AND DISCUSSION

Since the DSMC scheme used in the present study is a standard one, we omit its description for brevity (see, e.g., [4]) and show only the results. The following notation is used in this paper: ρ_{av} the average density over the ring (Problem I) or the entire cascade system (Problem II), l_0 the mean free path of the gas molecules in the equilibrium state at rest with density ρ_{av}, i.e., $l_0 = m/\sqrt{2}\pi d_m^2 \rho_{av}$ with m and d_m being the mass and diameter of a molecule, Kn$= l_0/w$ the Knudsen number, and R the specific gas constant (i.e., the Boltzmann constant divided by m).

Circulating flow

We first show some results for Problem I in the case of $T_1/T_0 = 3$ and $L/R_c = \pi$ (the length of the straight channel is equal to that of the median line of the semi-circular channel) for three different widths, i.e., $R_c/w = 1$ (Case 1), 2 (Case 2), and 5 (Case 3). Because of the symmetry, computation can be performed in the half part ABC of the circuit by imposing the condition that the velocity distribution function at B and that at D are symmetric with respect to the center of the ring O.

Figure 2 shows the flow-velocity field in the half part of the circuit at three different Knudsen numbers, Kn $= 0.2$, 1, and 5, for Case 1. In the figure, the arrow indicates the two-dimensional flow-velocity vector $\underline{\mathbf{v}}$ at its starting point. The length of the arrow corresponding to $0.01(2RT_0)^{1/2}$ [Figs. 2(a) and 2(b)] or $0.005(2RT_0)^{1/2}$ [Fig. 2(c)] is shown in the figure. Although its speed is low, a circulating flow in the counterclockwise direction is induced in the circuit. When Kn is relatively small (Kn $= 0.2$), the flow is rather localized; that is, the flow is limited to the vicinity of the inner wall in the semi-circular segment and to the middle part in the straight segment. For intermediate Kn (Kn $= 1$), the flow tends to spread over the channel. For larger Kn (Kn $= 5$), the flow becomes localized again, but in a different manner, that is, the flow is limited to the inner half of the straight segment but penetrates deeply in the outer half of the semi-circular segment.

Let us denote by $\mathscr{M}$ the mass-flow rate, per unit time and per unit thickness of the channel, of the counterclockwise circulating flow. The mass-flow rate per unit width of the channel, $\mathscr{M}/w$, versus Kn is shown in Fig. 3 for Case 1,
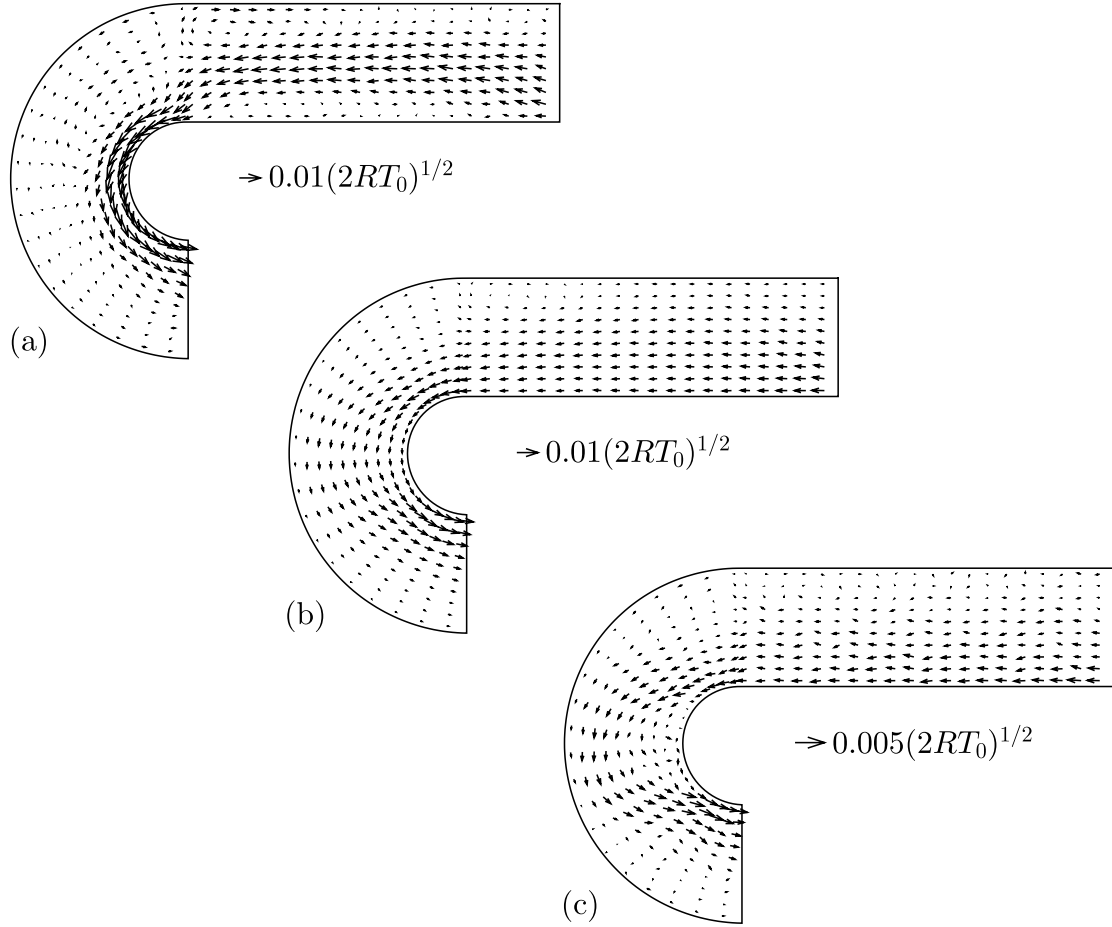
FIGURE 2. Flow-velocity field in the half part of the circuit. (a) Kn = 0.2, (b) Kn = 1, (c) Kn = 5.

Case 2, and Case 3. When the channel is thick (Case 1), the peak is at around Kn = 0.5. As the channel width decreases (Case 1 → Case 2 → Case 3), the mass-flow rate decreases, and the peak moves toward higher Kn. The numerical values corresponding to Fig. 3 are given in Table 1. The positions of the symbol □ at Kn = 0.1 and 0.2 of Case 2 in Fig. 3 appear to be unnatural. We will come back to this point later.

TABLE 1. Mass-flow rate versus Kn. The value in the parentheses is the result obtained by the use of a coarser cell system (see the second paragraph from the last in this subsection).

Kn	$[\mathscr{M}/\rho_{av}(2RT_0)^{1/2}w] \times 10^3$					
	Case 1		Case 2		Case 3	
0.1	1.54	(1.66)	0.436	(0.402)	—	
0.2	2.69	(2.91)	0.471	(0.434)	—	
0.5	3.41	(3.51)	1.12	(1.10)	0.127	(0.122)
1	2.75	(2.67)	1.61	(1.66)	0.314	(0.281)
2	1.78	(1.78)	1.54	(1.55)	0.578	(0.583)
5	0.844	(0.898)	1.04	(1.04)	0.724	(0.707)
10	0.455	(0.351)	0.636	(0.609)	0.620	(0.663)

The system for the present DSMC computation is as follows. The straight segment is divided into 160 (in the direction along the walls) × 50 (in the width direction) uniform cells in Case 1, 200 × 40 uniform cells in Case 2, and
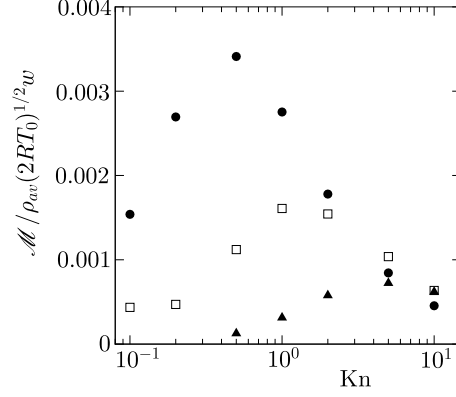
FIGURE 3. Mass-flow rate versus Kn. ●: Case 1, □: Case 2, ▲: Case 3.

360×24 uniform cells in Case 3. In each case, the semi-circular segment is divided into the same number of cells as the straight segment in such a manner that the size of the cells is almost uniform. The total number of simulation particles is 1.6×10^5 in Case 1 and Case 2 and 1.7274×10^5 in Case 3. The initial distribution is the stationary Maxwellian distribution with density ρ_{av} and temperature T_0. The time step Δt is $2t_0/\sqrt{\pi} \times 10^{-2}$ for Kn≤ 0.5 and $t_0/\sqrt{\pi}$Kn$\times 10^{-2}$ for Kn> 0.5, where $t_0 = (\sqrt{\pi}/2)(2RT_0)^{-1/2}l_0$ is the mean free time corresponding to l_0. The results shown above are the averages over more than $2 \times 10^6 \Delta t$ after the steady states are judged to have been reached. In each case, a computation using a system with coarser cells was also performed [the total number of cells is one fourth and that of the simulation particles is one eighth (exactly in Case 1 and Case 2 and almost exactly in Case 3) of the system mentioned above]. The mass-flow rate obtained by this system is shown in the square brackets in Table 1. In Case 3, the mass-flow rate is so small that it is impossible to obtain reliable values for small Knudsen numbers. The values at Kn = 0.1 and 0.2 of Case 2 in Table 1 show that there are still significant differences depending on the computational systems. Therefore, we need a much larger computation to obtain more accurate values that would give natural behavior in Fig. 3.

The mass-flow rate $\mathscr{M}$ is, theoretically, independent of the cross section of the channel. However, its numerical value shows small fluctuations depending on the cross section because of numerical error. The results shown in Fig. 3 and Table 1 are the averages over the straight segment. The variation from the average provides a measure of accuracy. In the computation using the system with finer cells, the standard deviation (in the straight segment) is less than 0.4% and 0.2% for Kn = 0.1 and 0.2, respectively, in Case 2, and it is less than 0.08% for all the other cases.

Pumping effect

We next consider Problem II in the case of $T_1/T_0 = 3$ and $L/R_c = \pi$. Let $\mathscr{N}$ be the number of the basic units, i.e., $\mathscr{N} = 1$ means the single unit P (with both ends being closed), $\mathscr{N} = 2$ means P + P$'$, and so on, and let s be the distance along the median line, $s = 0$ indicating the end of the first basic unit [the upper right end of the channel in Fig. 1(b)]. Therefore, the end $s = 0$ and $s = \mathscr{N}L_s$, where $L_s = L + \pi R_c$ is the length of the median line of the basic unit, are closed by the diffusely reflecting wall. Then, we define the average pressure $P(s)$ over the cross section that is perpendicular to the pipe wall and a semi-local Knudsen number Kn$_L(s)$ by $l_L(s)/w$, where $l_L(s)$ is the mean free path of the gas molecules in the equilibrium state at rest with density being the average density $\rho_{avL}(s)$ over the channel corresponding to the interval $[s, s+L_s]$, i.e., $l_L(s) = m/\sqrt{2}\pi d_m^2 \rho_{avL}(s)$. In this paper, we follow the idea of [4] how to estimate the pumping effect. In fact, the following description is similar to that in [5]. We note that the system with coarser cells (see the previous subsection) is used for the computation in this section.

Figures 4(a) and 4(b) show the distributions of $P(s)$ and Kn$_L(s)$ for Kn = 1 and $\mathscr{N} = 1, 2, 3, 5, 10,$ and 24 in the case corresponding to Case 1 ($R_c/w = 1$) in Problem I. The pressure rise is about 22.4% over ten basic units and about 60.2% over 24 basic units.

For a given set of the parameters $(L/R_c, R_c/w, T_1/T_0, \text{Kn}, \mathscr{N})$, the pressure ratio $P(s+L_s)/P(s)$ can be expressed as a function of Kn$_L(s)$ because Kn$_L(s)$ is monotonic in s. Figure 5(a) shows $P(\cdot + L_s)/P(\cdot)$ versus Kn$_L(\cdot)$ for $\mathscr{N} = 5, 10,$ and 24 in the case of $R_c/w = 1$ and Kn = 1. The data in the basic units at both ends $[0 \leq s < L_s$ and $(\mathscr{N}-1)L_s < s \leq \mathscr{N}L_s]$ are shown by smaller symbols. The data with larger symbols lie on a single curve irrespective
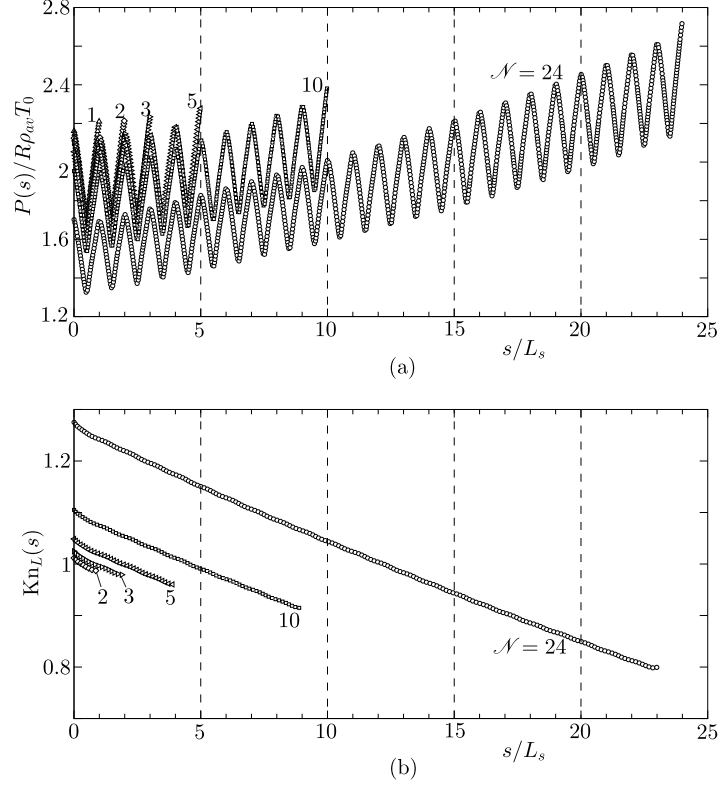
FIGURE 4. Distributions of $P(s)$ and $Kn_L(s)$. (a) $P(s)$, (b) $Kn_L(s)$.

of $\mathcal{N}$. The data with smaller symbols in the end units exhibit sharp projections upward and downward, which are attributed to the end effect. Therefore, it is limited to the first and the last unit. Taking into account this feature, we can obtain the curve $P(\cdot + L_s)/P(\cdot)$ versus $Kn_L(\cdot)$ for a wide range of $Kn_L(\cdot)$, instead of the computation for large $\mathcal{N}$, by joining the pieces of the curve obtained for a fixed $\mathcal{N}$ (say $\mathcal{N} = 12$) and different Kn. By this computation, the result for large $\mathcal{N}$ can be obtained by smaller computation. Figure 5(b) shows an example of the curve for $R_c/w = 1$, constructed with the data at Kn $= 0.22$, 0.26, 0.32, 0.4, 0.5, 0.6, 0.75, 1.35, and 1.6 for $\mathcal{N} = 12$ and at Kn $= 1$ for $\mathcal{N} = 24$. The result for each Kn can be identified as the part between the upward and downward projections with the value of Kn. From this curve and the curve of $Kn_L(\cdot + L_s)$ versus $Kn_L(\cdot)$ that are also shown in Fig. 5(b), one can estimate the compression ratio obtained when two reservoirs are connected by the cascade system composed of a large number (say $\mathcal{N}'$) of the basic units in the following way. Let $s = 0$ be the entrance of the low-pressure side and suppose that $P(0)$ and $Kn_L(0)$ are approximately given by the pressure and the local Knudsen number there. Then, by reading the values of the pairs $[P(L_s)/P(0), Kn_L(L_s)]$, $[P(2L_s)/P(L_s), Kn_L(2L_s)]$, ..., $[P(\mathcal{N}'L_s)/P((\mathcal{N}'-1)L_s), Kn_L(\mathcal{N}'L_s)]$ successively from the figure, we can obtain the total compression ratio $P(\mathcal{N}'L_s)/P(0)$ by simple multiplications. This is the approximate compression ratio between the reservoirs. For example, the cascade system composed of sixty basic units gives compression ratio about 3 when $Kn_L(0) = 1 \sim 1.5$.

In conclusion, if many units are used, the cascade system shown in Fig. 1(b) (with a periodic temperature distribution) acts as a pump that gives a significant compression ratio.
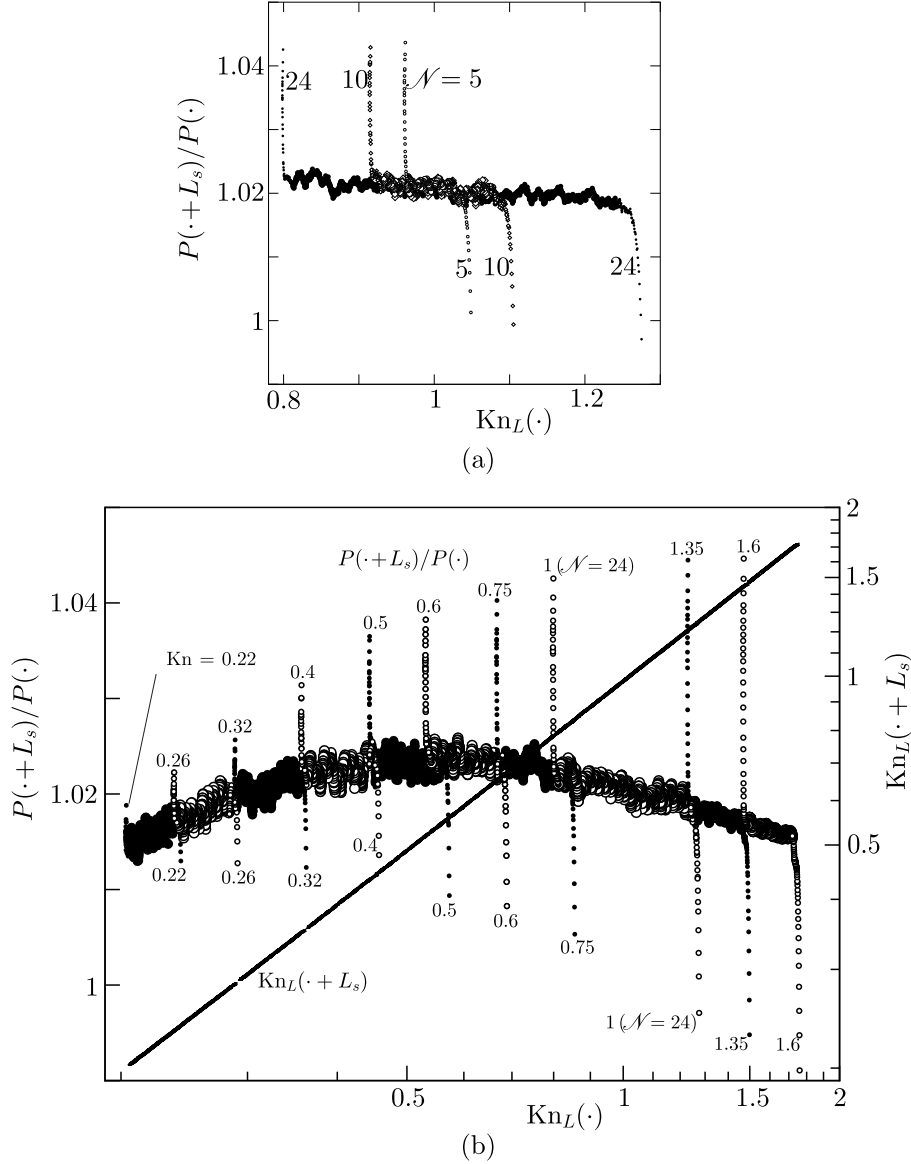
ACKNOWLEDGMENTS

FIGURE 5. $P(\cdot + L_s)/P(\cdot)$ and $Kn_L(\cdot + L_s)$. (a) $P(\cdot + L_s)/P(\cdot)$ vs $Kn_L(\cdot)$ for $\mathcal{N} = 5$, 10, and 24, (b) $P(\cdot + L_s)/P(\cdot)$ vs $Kn_L(\cdot)$ for many values of Kn together with $Kn_L(\cdot)$ vs $Kn_L(\cdot)$.

REFERENCES

1. Knudsen, M., Ann. Phys. **31**, 205 (1910).
2. Sone, Y., *Kinetic Theory and Fluid Dynamics*, Birkhäuser, Boston, 2002.
3. Sone, Y. and Yamamoto, K., Phys. Fluids **11**, 1672 (1968).
4. Sone, Y., Waniguchi, and Aoki, K. Phys. Fluids **8**, 2227 (1996).
5. Aoki, K., Sone, Y., Takata, S., Takahashi, K., and Bird, G. A., in *Rarefied Gas Dynamics*, edited by Bartel, T. J. and Gallis, M. A., AIP, Melville, 2001, p. 940.
6. Bird, G. A., *Molecular Gas Dynamics*, Oxford University Press, Oxford, 1976.
7. Bird, G. A., *Molecular Gas Dynamics and the Direct Simulation of Gas Flows*, Oxford University Press, Oxford, 1994.
8. Sone, Y. and Sugimoto, H., in *Rarefied Gas Dynamics*, edited by Muntz, E. P. and Ketsdever, A., AIP, Melville, 2003, p. 1041.
9. Han, Y. L., Young, M., Muntz, E. P., and Shiflett, G., in *Rarefied Gas Dynamics*, edited by Capitelli, M., AIP, Melville, 2005, p. 162.
10. Aoki, K., Degond, P., Mieussens, L., Takata, S., and Yoshida, H., in preparation.